Gamma-TuRC proteins contribute to the dynamic organization of MTOCs during *Drosophila* spermatogenesis

Elham Alzyoud[1#], Dóra Németh[1,2#], Viktor Vedelek[1], Titanilla Szögi[3], Mónika Krecsmarik[1], Zoltán Lipinszki[4*], Rita Sinka[1*]

[1]Department of Genetics, University of Szeged, Szeged, Hungary
[2]Faculty of Science and Informatics, Doctoral School of Biology, University of Szeged, Szeged, Hungary
[3]Department of Pathology, University of Szeged, Szeged, Hungary
[4]HUN-REN Biological Research Centre, Institute of Biochemistry, MTA SZBK Lendület Laboratory of Cell Cycle Regulation, Szeged, Hungary

# These authors contributed equally to this work
* Authors for correspondence (rsinka@bio.u-szeged.hu, lipinszki.zoltan@brc.hu)

Abstract

The initiation of microtubule formation in eukaryotes is primarily facilitated by γ-tubulin and the highly conserved protein complex called γ-Tubulin Ring Complex (γ-TuRC) in various microtubule-organizing centers (MTOCs). Non-centrosomal MTOCs have a range of functions and contribute to diverse cellular activities in different cell types. While the heterogeneity of tissue-specific MTOCs and γ-TuRC in *Drosophila* testis has been described, their molecular composition and physiological significance are poorly understood. In this study, we investigate the testis-specific distribution of the canonical γ-TuRC by *in vivo* tagging of two complex members, Grip163 and Grip84. We find that both the testis-specific (t- γ-TuRC) and canonical form of γ-TuRC are simultaneously present and colocalize with each other at the basal body, apical nuclear tip, and near the elongating mitochondrial derivatives in the post-meiotic spermatids. We propose the possibility of the formation of MTOCs containing both t-γ-TuRC and γ-TuRC complexes. We also find some of the known γ-TuRC binding partners localizing to the apical nuclear tip. Additionally, we identify the Golgi localization of Grip84 in spermatocytes, alongside its centrosomal and diverse post-meiotic localization. These results highlight and prove the importance of the different γ-TuRCs in organizing the diverse MTOCs during the extensive rearrangement of cell organelles in *Drosophila* spermatogenesis.

Introduction

The microtubule (MT) network in eukaryotic cells plays a crucial role in cell differentiation and division, as well as movement through the cilia and flagella. The spatial re-organization of the MT cytoskeleton is a fast and dynamic process that requires distinct subcellular nucleation sites called microtubule organizing centers (MTOCs) that act as templates for the MT arrays to initiate. The main MTOC in dividing cells is the centrosome, which consists of a pair of centrioles (an older mother and a newer daughter centriole), and the pericentriolar material (PCM). When cells exit the cell cycle and start differentiation, their centrosomes become inactive, resulting in a gradual loss of their MTOC activity [1]. To support different functions and structures, the cells employ a variety of non-centrosomal MT organizing centers (ncMTOCs) [2]. The heterogeneity of ncMTOCs is reflected in the molecular composition and the cellular localization, and their function is unique to each cell type [3].

MTs are polar structures containing a plus and a minus end. The highly dynamic plus end is generally where the majority of MT polymerization and depolymerization occurs, while the minus end is often stabilized and capped [4]. The main factor known to specifically associate with microtubule minus ends is the γ-tubulin ring complex (γ-TuRC) [5,6]. PCM and ncMTOCs both recruit γTuRCs to the microtubule nucleation site [7,8]. γTuRC is a multiprotein complex consisting of γ-tubulin and its associated proteins (γ-tubulin ring proteins (Grips) in Drosophila, or γ-tubulin complex proteins (GCPs) in human) that are essential for γTuRC integrity and MT nucleation activity. The conserved and essential core of the γTuRC is the small complex (γTuSC) that consists of two γ-tubulins and one copy of Grip84 and Grip91 in Drosophila [9]. The large ring complex comprises multiple γ-TuSCs and additional Grips, including Grip75, Grip128, Grip163, and Grip71 [10,11] and is able to nucleate microtubule organization more efficiently than the small complex.

Similarly to mammals, Drosophila spermatogenesis involves a series of stage-dependent morphological changes when stem cells give rise to mature sperm. During this process, round spermatids of 10 μm in diameter elongate to become 1850 μm in length [12], which requires an extensive remodelling of existing cellular organelles, as well as the addition of new structures. After meiosis, each spermatid inherits a centriole that will serve a basal body around a ring-shaped PCM-like macromolecular structure called the centriole adjunct. The growth of the axoneme starts from the basal body and continues to elongate towards the spermatid tail [13]. Opposite to the basal body, on one side of the nucleus, the acroblast starts to develop, which is a Golgi-derived organelle. During the later stages of elongation, the acroblast will be converted

69 into the acrosome. Another important event that occurs after meiosis is the fusion of the mitochondria into
70 two giant mitochondrial derivatives, called the nebenkern. These mitochondrial derivatives elongate with
71 the axoneme during sperm maturation and accumulate paracrystalline material in one of them, which could
72 provide structural support for the growing tail [12,14].
73 Growing evidence suggests that testis-specific MTOC components play important roles in basal body and
74 ncMTOC formation and also in the positioning and shaping of the post-meiotic organelles during
75 Drosophila spermatogenesis [15–17]. For instance, testis-specific CnnT expression contributes to the
76 conversion of mitochondria into a ncMTOC, independent of core pericentriolar Cnn [16]. In addition to the
77 canonical γ-TuRC genes (Grip84, Grip91, Grip75, Grip128, Grip163, and Grip71), recently we have
78 identified three additional testis-specific paralogs of the γ-TuRC components, t-Grip84, t-Grip91, and t-
79 Grip128 [15,18]. We have shown, that from the round spermatid stage onward, these t-γ-TuRC proteins start
80 to localize to the centriole adjunct, then to the nuclear tip, and finally surrounding the mitochondria of the
81 elongating cyst. We also presented that they bind to γ-Tubulin and Mzt1 and interact with each other in
82 the post-meiotic stages [15]. We and others have shown that Mzt1 binds to the N-termini of the GCP proteins
83 (Zupa et al., 2021) and interacts with the N-terminal regions of Grip91, t-Grip91 and Grip128 in
84 Drosophila [15,17]. Our finding raised the question of whether the canonical γ-TuRC proteins are replaced
85 with their testis-specific counterparts, or whether they are able to cooperate to meet the needs of ncMTOCs
86 during the late stages of spermatogenesis. We also aimed to understand whether the testis-specific γ-TuRC
87 can interact with the canonical γ-TuRC or with any other proteins. In order to address these queries, we
88 created *in situ* tagged *Grip163* and *Grip84* transgenic lines to elucidate the adaptable localization and
89 identify interacting partners of the γ-TuRC during the development of germ cells.
90
91 **Results**
92 **Phenotypic characterization of the *Grip163*$^{\Delta 11}$ mutant line**
93 We have previously reported that t-γ-TuRC proteins are present only in the post-meiotic spermatids [15].
94 However, there is a lack of data regarding the relationship between the canonical and the testis-specific γ-
95 TuRCs, as well as the presence or localization of ubiquitously expressed γ-TuRC components in the late
96 stages of spermatogenesis.
97 Therefore, we tested the presence and possible function of the γ-TuRC component Grip163, which has no
98 testis-specific paralogs, in sperm development [19,10,15]. To achieve this, we induced mutation in the *Grip163*
99 gene, and performed an *in situ* tagging of the *Grip163* gene, using the CRISPR-Cas9 gene editing

100 technology. Using a specific guided RNA designed for *Grip163*, we deleted 11 base pairs from the coding
101 region of the gene (hereafter, *Grip163*$^{\Delta 11}$). This deletion caused a frameshift leading to a premature stop
102 codon in the coding region of *Grip163* (**S.Figure 1a**). Interestingly, we found that in contrast to the G*rip84*
103 and *Grip91* homozygotes, which are lethal [20,21], the homozygous *Grip163*$^{\Delta 11}$ mutant animals are viable,
104 but male and female sterile (**S.Figure 1c).** The seminal vesicles of the *Grip163*$^{\Delta 11}$ males were empty,
105 without mature sperms (**Figure 1 a-b**). A very similar phenotype was observed in *Grip128* and *Grip75*
106 (γ-TuRC components) mutants [22].
107 Based on this phenotype we investigated both the early and late stages of spermatogenesis in
108 *Grip163*$^{\Delta 11.}$flies. We found an abnormal nebenkern-nucleus ratio in the round spermatids, which is a
109 hallmark of abnormal mitotic division (**Figure 2 a-c)**. Nevertheless, many of the cysts are able to elongate
110 in the *Grip163*$^{\Delta 11}$ mutant, visualized by the β2tub-GFP transgene (**Figure 1 a, b)**. To further investigate
111 the elongation of the cysts, we tested whether the individualization proceeds normally. To visualize every
112 elongated post-meiotic cyst, we stained the actin cones of the individualization complex (IC) in the
113 *Grip163*$^{\Delta 11}$ testis and found the lack of IC in *Grip163*$^{\Delta 11}$, providing evidence for the failure of proper cyst
114 elongation, which is the prerequisite of individualisation **(Figure 1 c, d).** For further evidence, we used
115 anti-pan polyglycylated tubulin (Axo49) antibody to visualize mature axonemes of the spermatids, at the
116 onset of individualization [23]. We observed significantly shorter axonemes in the *Grip163*$^{\Delta 11}$ mutant
117 compared to the WT, indicating abnormal spermatid elongation **(Figure 1 e-g).** Axoneme elongation
118 depends on the mitochondria, which provide a structural platform for MT reorganization to support the
119 robust elongation taking place at the tip of the sperm tail (Nouguchi 2011). Based on this we tested the
120 presence and appearance of late elongating mitochondria using dj-GFP as a marker. In accordance with
121 the defect observed in axoneme elongation, it was detected that the mitochondria in the *Grip163*$^{\Delta 11}$
122 mutants also exhibited incomplete elongation (**Figure 1 e, f**). Based on this general spermatid elongation
123 defect of *Grip163*$^{\Delta 11}$ flies, the detailed morphology of post-meiotic cysts was further investigated using
124 transmission electron microscopy (TEM).
125 In wild-type testis, the 64 spermatids develop simultaneously and on the TEM image of elongated cysts
126 we observed the two mitochondrial derivatives attached to the axoneme, which has the classical 9+2
127 arrangement of microtubules in each spermatid (**Figure 2 d-h**). In *Grip163*$^{\Delta 11}$ mutants, cysts became
128 disorganized, with fewer spermatids per cyst and with disturbed mitochondrial:axonemal ratio **(Figure 2**
129 **b).** Frequently, multiple mitochondrial derivatives were attached to a single axoneme, and we also
130 observed multiple damaged axonemes **(Figure 2 h)**, supporting that Grip163 is necessary for normal

131 axoneme formation and/or stability. Since the γ-TuRC is essential for centrosome formation [11,20,24,25], we
132 examined the centrosome/basal body distribution at different stages of spermatogenesis in the testes of
133 *Grip163*$^{\Delta 11}$ males. We tested the distribution of the centrosomal/basal body localized γ-Tubulin and the
134 PACT domain of DPlp fused with GFP (GFP-PACT) [26]. In the wild type animals both proteins localize to
135 the centrosome/basal body during different stages of spermatogenesis **(Figure 3 a, b)**. In the *Grip163*$^{\Delta 11}$
136 mutant flies we found strong GFP-PACT positive centrosomal and basal body signals, but the γ-Tubulin
137 signal in spermatocytes and spermatids was weak compared to the wild type **(Figure 3 c, d)**. In wild type
138 males, GFP-PACT is located close to the nucleus and the nebenkern, as expected in round spermatids. In
139 contrast, multiple and scattered GFP-PACT signals were observed in the *Grip163*$^{\Delta 11}$ mutants' testis
140 (**Figure 3 c-d)**. We could detect γ-Tubulin in the post-meiotic elongating spermatids, but those were
141 scattered along the cysts of *Grip163*$^{\Delta 11}$ mutant (**Figure 3 c, d**). All these data suggest that Grip163 could
142 be essential for the formation of stable γ-TuRC prior to and at the onset of meiosis, however, the newly
143 organized testis-specific γ-TuRC could contribute to the γ-Tubulin binding after meiosis.
144 Interestingly, mutants of the canonically expressed γ-TuRC components, *Grip128* and *Grip75,* are also
145 viable and sterile with scattered basal body distribution [22]. Contrary to the essentiality of γ-TuSC genes,
146 the absence of the additional complex members contributing to the formation of γ-TuRC, is not critical
147 for viability, but they are required for normal fertility in both sexes [22].
148
149 **Localization of γ-TuRC proteins during spermatogenesis**
150 To test the subcellular localization of Grip163 at different stages of spermatogenesis, we generated
151 endogenously GFP-tagged Grip163 lines. We and others have shown that the N- or C-termini of the γ-
152 TuRC proteins are responsible for the binding of their interacting partners [15,17], therefore we tagged the
153 Grip163 close the N-terminus, without interfering with the functional GCP domains of the protein
154 (**S.Figure 1 a**). The fertility of the GFP-Grip163 males was comparable to the wild-type animals,
155 indicating that the inserted fluorophore does not alter the function of the protein (**S.Figure 1 c)**.
156 GFP-Grip163 signal was present on the centrosomes of spermatocytes and after meiosis, it appeared on
157 the basal body/centriole adjunct of the developing spermatids as well **(Figure 4 a-e)**. Similar to the testis-
158 specific γ-TuRC members, GFP-Grip163 was also detected at the apical end of the nuclei and
159 accumulation was observed at the mitochondrial surface (**Figure 4 d, e**). These results strongly suggest
160 that the testis-specific γ-TuRC does not replace the canonical γ-TuRC, but both are present and form
161 similarly distributed versatile ncMTOCs in the post-meiotic spermatids.

162 The localization of GFP-Grip163 to the centriole adjunct has prompted an inquiry into the potential
163 presence of other canonical γ-TuSC components in the subsequent developmental stages. To investigate
164 this, we applied CRISPR technology to *in situ* tag Grip84 with GFP. We designed the incorporation in a
165 way that all 5 potential isoforms of Grip84 will have the N-terminally inserted GFP tag, outside of the
166 GCP domain (**S.Figure 1 b**). It was previously reported that the classical mutant of *Grip84* is lethal,
167 therefore the normal viability and fertility of the *in situ* GFP-tagged Grip84 serves as evidence that the
168 GFP tag does not alter the normal function of Grip84 (**S.Figure 1 c**) [27].
169 We found that GFP-Grip84 is present on the centrosomes of spermatocytes, similarly to the GFP-Grip163
170 protein (**Figure 5 a-e**).
171 This localization of GFP-Grip84 was also verified by its colocalization with the centrosomal component
172 Asterless (Asl) (**Figure 6 a, S.Figure 2 a, b**) [28].
173 Following meiosis, GFP-Grip84 is present on the centriole adjunct and then appears at the apical nuclear
174 tip tip and exhibits a strong overlap with the elongated mitochondria, akin to the GFP-Grip163. We wanted
175 to know whether the post-meiotic localization of GFP-Grip84 overlaps with its testis-specific paralogue,
176 t-Grip84. To do this we co-expressed GFP-Grip84 and t-Grip84-mCherry together and found complete
177 colocalization after the meiotic stages (**Figure 5 f, g**) [15]. These results provide additional evidence that
178 both the ubiquitously expressed γ-TuRC and the testis-specific γ-TuRC may together play a role in the
179 formation of the diverse microtubule organizing centers in post-meiotic stages of spermatids.
180 Apart from the centrosomal localization of GFP-Grip84, we also noticed strong bright punctae in the
181 cytoplasm of spermatocytes, whose distribution is reminiscent of t-ER-Golgi units. It is known that
182 centrosomal proteins are associated with the Golgi apparatus in mammalian cells [29]. Golgi organization is
183 special in Drosophila, as the scattered Golgi stacks are found in close proximity to the ER exit sites (t-ER-
184 Golgi) [30]. To test the t-ER-Golgi localization of GFP-Grip84, we used GM130 as a *cis*-Golgi, as well as
185 GCC88, as a *trans*-Golgi-specific antibody for co-immunostaining (**Figure 6 b-e, S.Figure 2 c-d**). We
186 observed strong co-localization of GFP-Grip84 with the *cis*-Golgi, suggesting that GFP-Grip84 is
187 connected to the t-ER-Golgi units of spermatocytes.
188 In a comprehensive analysis of the effector proteins of Rab GTPases, Grip84, Grip91 and γ-Tubulin were
189 identified as interacting partners of the Golgi-localizing Rab2 and Rab4 [31]. Rab2A and Rab2B proteins
190 were shown to be essential for acrosome formation and male fertility in mice [32], therefore it seemed
191 reasonable to check whether the Golgi-localizing Rab2 might also be present at the apical end where the
192 acrosome is located during nuclear elongation in Drosophila spermatids. We tested the germline-specific

193 Bam-Gal4 driven pUASP-Rab2-YFP localization in spermatocytes and spermatids. We detected Rab2-
194 YFP on the t-ER-Golgi units adjacent to the *trans*-Golgi-specific antibody GCC88 in spermatocytes and
195 on the acrosome containing apical nuclear tip of the elongated spermatids (**Figure 6 d, e**). Localization of
196 GFP-Grip84 to the Golgi apparatus led us to hypothesize that Drosophila γ-TuRC, similarly to the
197 mammalian γ-TuRC is necessary to the Golgi organization and also raised the possibility of a conserved
198 function of Rab2 in acrosome formation. Additional experiments can address these highly intriguing
199 prospects.
200
201 **Post-meiotic ncMTOCs contain centrosomal components**
202 The versatile localization pattern of GFP-Grip84 prompted us to investigate whether any of the already
203 known binding partners of the γ-TuRC could be present on the newly identified localization foci. It was
204 shown previously that γ-Tubulin is localized in the apical region of the spermatid nuclei, specifically at
205 the distal end of the MTs present within the dense complex [15,33]. We previously demonstrated the presence
206 of t-γ-TuRC and Mtz1 at the apical tip of the nucleus, suggesting the presence of a ncMTOC organized
207 opposite to the basal body during nuclear elongation [15]. Therefore, we carefully examined the precise
208 localization of the centriole component, Sas4, a known interacting partner of γ-TuRC proteins by
209 immunostaining using anti-Sas4 antibody [34,35]. We detected Sas4 on the centrosome of mitotic
210 spermatocytes and the basal body of the spermatids after meiosis (**Figure 7 a-c**). Intriguingly, we detected
211 endogenous Sas4 on the apical tip of the elongating spermatid nuclei as well (**Figure 6 c**). Apart from the
212 γ-TuRC proteins, Sas4 has multiple centriolar binding partners, including Sas6, Asl, Ana1, and Dplp [28,35–
213 38]. Therefore, we wondered whether they are also present on the ncMTOC at the apical tip of the spermatid
214 nuclei. To achieve this we performed immunostaings using gene-specific antibodies [28,34,39]. We detected
215 Sas6 and Asl on the centriole adjunct and also at the apical tip of the nuclei (**S.Figure 3 a, b**), however,
216 Ana1 and GFP-PACT colocalized with t-Grip91 exclusively at the centriole adjunct region of the
217 elongating leaf and canoe stage nuclei, in line with the reported localization pattern of these proteins [33]
218 (**Figure 7 d, S.Figure 3 c**). These results indicate that the ncMTOC localised to the apical nuclear tip
219 contains several well-defined binding partners of the γ-TuRC.
220
221 **Composition of t-γ-TuRC**
222 We next examined whether the partially overlapping localization pattern might be a consequence of the
223 physical interaction between the canonical γ-TuRC and the t-γ-TuRC and/or the t-γ-TuRC proteins and

224 the γ-TuRC interacting protein Sas4. To address this, we performed a yeast two-hybrid (Y2H) analysis,
225 where we tested t-γ-TuRC proteins with the canonical γ-TuSC protein Grip91 and Sas4. Due to the large
226 size of the proteins, we divided all three t-γ-TuRC proteins and Grip91 into an N-terminal (N) and a C-
227 terminal (C) part. We found a specific interaction between t-Grip84-C and Grip91-N, which suggests the
228 possibility of the presence of a testis-specific and non-testis-specific mixed γ-TuRC (**Figure 8 a, S.Figure**
229 **4**). We also detected interaction between Sas4 and t-Grip91-N, t-Grip91-C, t-Grip128-N and t-Grip128-C
230 however, we could not find an interaction between Sas4 and t-Grip84-N, t-Grip84-C (**Figure 8 a, S.Figure**
231 **4**). To support Y2H results and prove the direct binding between proteins, we performed *in vitro* binding
232 experiments. We used immobilised GST-tagged recombinant proteins (N- or C-terminal parts of the t-γ-
233 TuRC proteins, as indicated) as bait, which were mixed with ^{35}S-methionine-labelled Sas4 or Grip91,
234 respectively, produced by a coupled *in vitro* transcription-translation (IVTT) reaction followed by
235 autoradiography (**Figure 8 b-e**). The *in vitro* binding experiments confirmed the results of the Y2H assay
236 (**Figure 8 a-e**). Taken together the *in vivo* localization pattern and the *in vitro* interaction results suggest
237 a versatile γ-TuRC containing ncMTOC formation in Drosophila spermatids.
238

239 **Discussion**

240 Drosophila spermiogenesis and spermatogenesis represent an ideal model for studying mitotic and meiotic
241 cell division, centrosome and basal body formation and dynamic organelle reorganization after meiosis.
242 It was proven to be a good model for understanding centrosomal and non-centrosomal MT nucleation due
243 to the intensive morphological changes and organelle movement in the post-meiotic spermatids [15–17]. MT
244 nucleation was reported, among others, at the surface of the Golgi [40], mitochondria [16], nuclear envelope [41]
245 and plasma membrane [42] in mammalian cells. We previously identified and described the function and
246 versatile localization of three testis-specific γ-TuRC proteins in the post-meiotic spermatids [15](**Figure 9**).
247 The described centriole adjunct, nuclear tip and mitochondrial surface localization of the t-γ-TuRC
248 proteins and their interaction partner Mzt1 raised the question of whether the ubiquitously expressed γ-
249 TuRC is replaced after meiosis for the testis-specific one or both are present due to the multiple ncMTOC
250 formation during spermatid elongation and acrosome formation. γ-Tubulin was already reported to
251 localize to both tips of the elongating nuclei and to the surface of the giant mitochondria during elongation
252 [15,16,33]. The testis-specific splice variant of Centrosomin (Cnn), CnnT, was also reported to promote non-
253 centrosomal MT growth on the surface of the mitochondrial derivative of spermatids [16]. However, we
254 lacked the canonical γ-TuRC localization after the meiotic stages of spermatogenesis, despite both CnnT

255 and γ-Tubulin can bind to γ-TuRC proteins. Mutants for the small complex components Grip91 and
256 Grip84 are lethal and have defects in spindle assembly [20,21], which indicates their essentiality for the whole
257 fly development. It has been demonstrated that the small complex is the minimal unit needed for MT
258 nucleation [9]. However, RNAi depletion of the ubiquitously expressed Grip163 results in loss of Grip84
259 recruitment to the ncMTOC in tracheal cells [11].
260 Our experiments showed that, in contrast to the essentiality of the γ-TuSC, the γ-TuRC member Grip163
261 is only essential for fertility, similar to the already characterized γ-TuRC members Grip75 and Grip128
262 [22]. From the elongation and basal body stability defects of *Grip163* mutant spermatids, we inferred that
263 the presence of Grip163 protein is essential after meiosis. This was supported by the localization of GFP-
264 Grip163, as we detected its presence in the localization foci of t-γ-TuRC members after meiosis. These
265 results raised the possibility that t-γ-TuRC and the canonical γ-TuRC may be present simultaneously, even
266 as a mixed complex, in the aforementioned ncMTOCs (**Figure 9**). This hypothesis was further supported
267 by the fact that Grip84, a member of γ-TuSC, also exhibits an overlapping localization pattern in the late
268 stages of spermatogenesis and the physical interaction between t-Grip84 and the ubiquitously expressed
269 Grip91. Our results strongly suggest that both testis-specific and canonical γ-TuRC members are involved
270 in the formation of post-meiotic ncMTOCs.
271 *In vivo* tagging of Grip84 enabled us to describe the Golgi localization of the γ-TuSC component Grip84
272 in primary spermatocytes, in addition to the extensively studied centrosomal localization of the Grip84 [21].
273 Until now γ-Tubulin containing Golgi outpost-associated MT nucleation sites was only described to
274 regulate distal dendritic branching in *Drosophila* neurons [43]. Golgi non-centrosomal MT assembly is
275 mediated by the γ-Tubulin-interacting AKAP450 protein, which is anchored by the cis-Golgi-associated
276 GM130 protein. This provides evidence that the Golgi apparatus may become a major site of MT
277 nucleation by acting as a γ-TuRC docking site in mammalian cells by a mechanism similar to that in the
278 centrosome (Rivero et al., 2009). Our results suggest that a similar mechanism could be present in the
279 primary spermatocytes. Further experiments are needed to determine exactly which isoform of the Grip84
280 protein is associated with the Golgi (**Figure 9**).
281 All three proteins of γ-TuSC (Grip84, Grip91 and γ-Tubulin) interact with the constitutively active, GTP-
282 bound Rab2 protein [31], and Rab2 and Grip84 both localize to both the Golgi and the apical end of the
283 nucleus, suggesting a role for γ-TuSC and Rab2 in the formation of the Golgi and lysosome-associated
284 acrosome. Rab2A and Rab2B proteins were shown to be components of the proacrosomal membrane and
285 essential for acrosome formation and male fertility in mice [32].

286 Drosophila Rab2 is an essential gene and recruitment of Rab2 takes place on the membranes of late
287 endosomes, where it controls the fusion of LAMP-containing biosynthetic carriers and lysosomes to late
288 endosomes in somatic cells [44]. t-ER-Golgi units contribute to the formation of the acroblast, which forms
289 the acrosome by fusing lysosomal structures during nuclear elongation in Drosophila [45]. The molecular
290 determinants of acrosome formation are hardly known in Drosophila, however, several retrograde
291 tethering complexes were described in the formation of a functional Golgi ribbon in the acroblast (Fári et
292 al 2016). Acrosomal proteins such as Sneaky, Lamp1 and Rab2, as well as the ubiquitous and testis-
293 specific γ-TuRC, its partner proteins (Mzt1, Sas4) and other centrosomal proteins (Asl, Sas6), are all
294 localized to the apical tip of the nucleus. Further biochemical studies are needed to clarify the precise
295 interactions between the aforementioned proteins. Nevertheless, these results raise the possibility of a link
296 between the ncMTOC and acrosome organization, which is present at the dense complex forming
297 perinuclear MTs at the apical end of the nuclei(**Figure 9**).
298

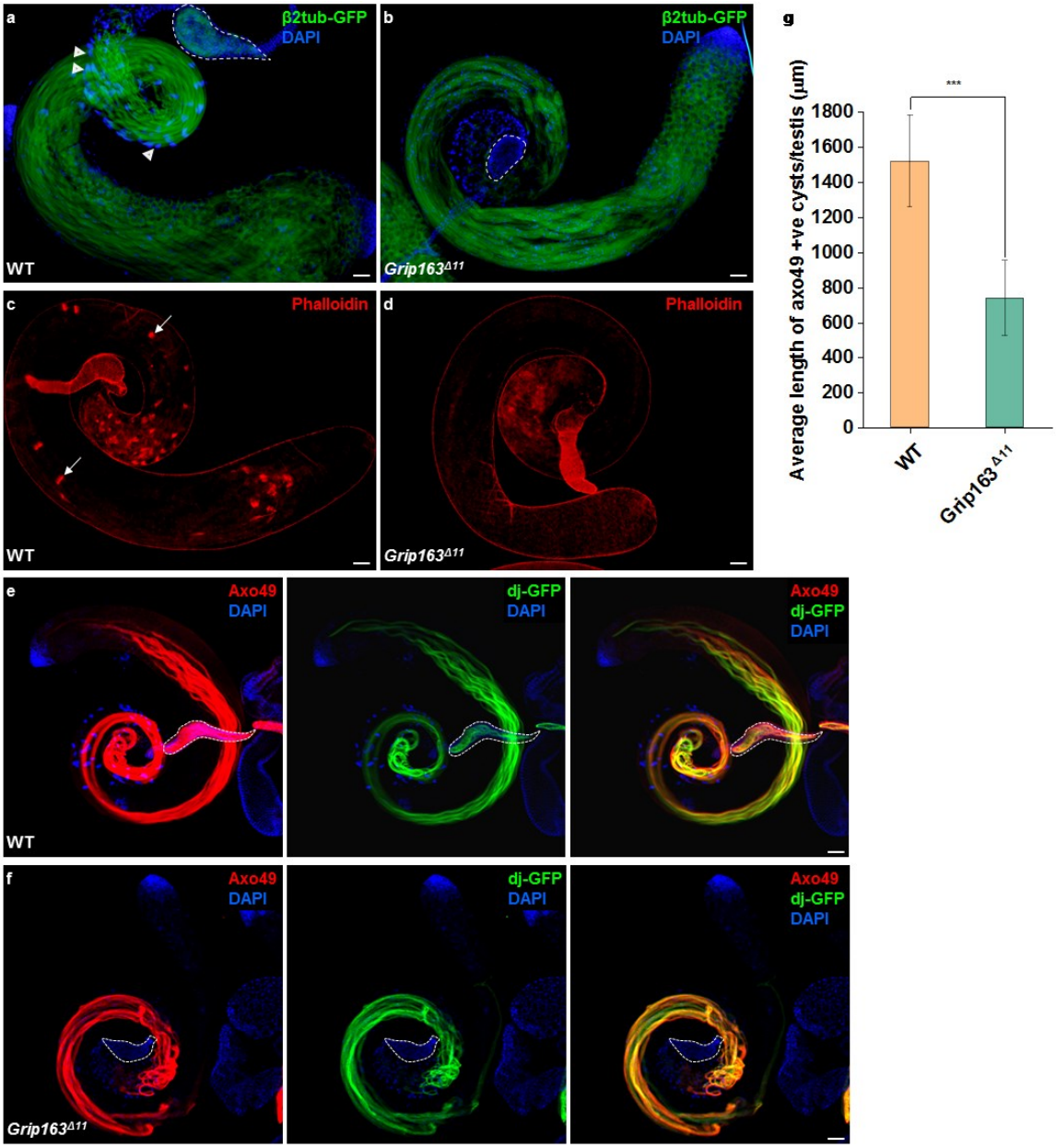

Figure 1. Mitochondrial and axonemal abnormalities lead to abnormal spermatid elongation in *Grip163$^{\Delta 11}$* mutant

(a, b) Microtubules are visualized with the β2tub-GFP transgene (green), while the nuclei stained with DAPI (blue) in WT **(a)** and *Grip163$^{\Delta 11}$* mutant spermatids **(b)** Elongated cysts are present both in WT and *Grip163$^{\Delta 11}$*, however, the seminal vesicle (dashed lines) of *Grip163$^{\Delta 11}$* mutant does not contain β2tub-GFP positive mature sperms. **(c, d)** The individualization complexes (IC) were stained with Phalloidin (red), ICs are formed normally (arrows) in WT, **(c)** and missing in *Grip163$^{\Delta 11}$* mutant **(d)**. **(e, f)** Fully developed axonemes are visualized by Axo49 tubulin antibody (red) and elongated mitochondria are with DJ-GFP transgene (green) both in the testis and seminal vesicle (dashed line). Elongated polyglycylated axonemes and mitochondria were shorter in *Grip163$^{\Delta 11}$* mutant and the seminal vesicle was empty (dashed line) **(f)** compared to the WT **(e). (g)** Diagrams show the average length of Axo49 positive cysts in WT and *Grip163$^{\Delta 11}$* mutant. (WT n=12, *Grip163$^{\Delta 11}$* n=22) Statistical significance was tested by one-way ANOVA. (scale bars: 50 µm).

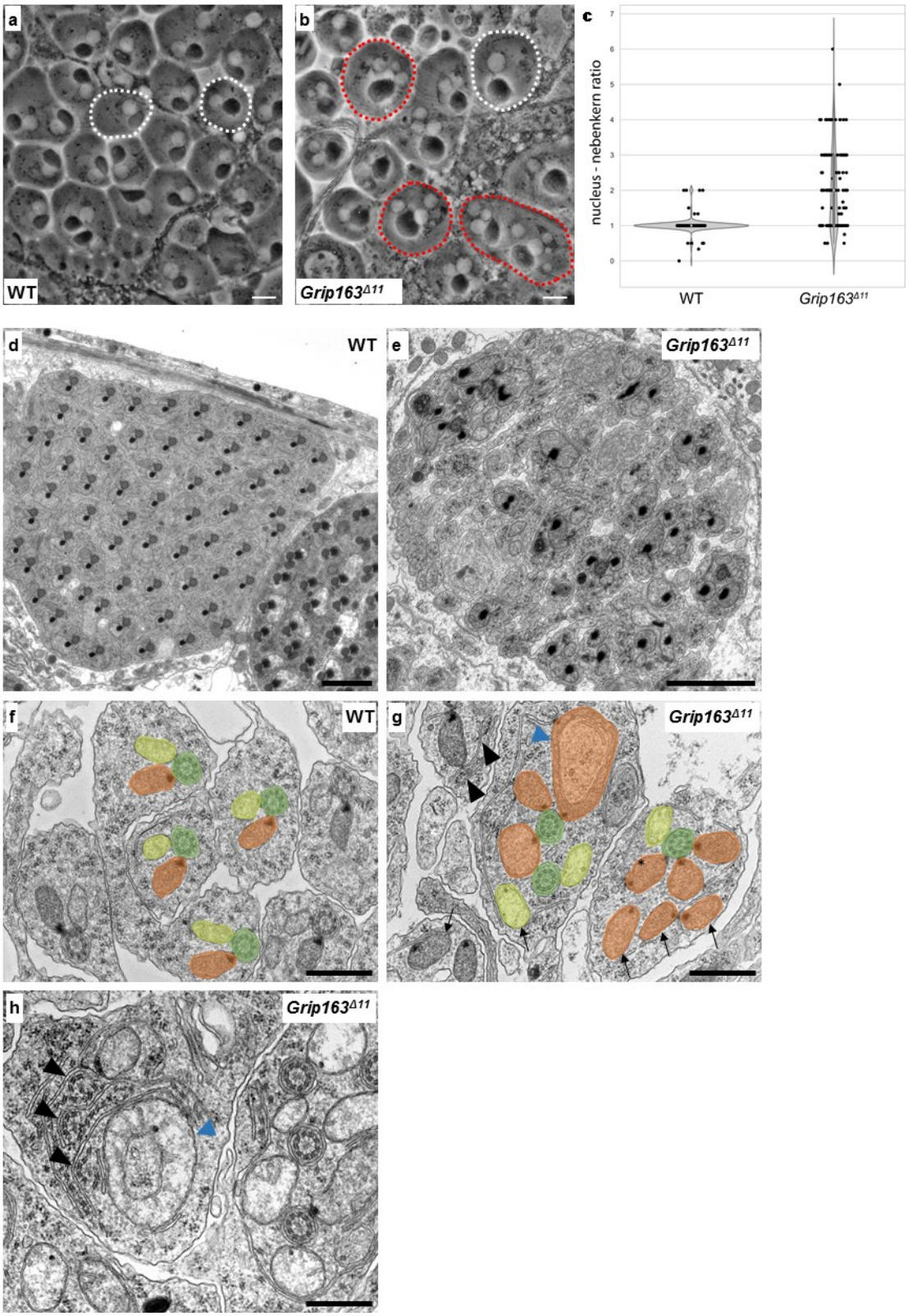

Figure 2: Abnormal mitochondrial and axonemal structures in the post-meiotic cysts of *Grip163$^{\Delta 11}$* mutant

316 **(a, b)** Phase contrast images show a normal 1:1 (white outline), nucleus: nebenkern ratio in WT **(a)** and
317 an abnormal ratio (red outline) in *Grip163*$^{\Delta 11}$ mutant **(b)**. **(c)** Violin plot showing the nucleus: nebenkern
318 ratio in WT (n=186) and *Grip163*$^{\Delta 11}$ mutant round spermatids (n=112). **(d, h)** Transmission electron
319 micrograms of testis cross-sections, representing elongating cysts of WT (**d,f**) and *Grip163*$^{\Delta 11}$ mutant
320 (**e,g,h**). Disorganized cysts with axonemal and mitochondrial abnormalities are characteristic in
321 *Grip163*$^{\Delta 11}$ mutant **(f-h)** WT elongating cyst shows normal axoneme structure with 9+2 tubulin dimers
322 (highlighted in green) and two mitochondrial derivatives (yellow and orange), with paracrystalline
323 material formation in one of them (orange) **(f)**. In *Grip163*$^{\Delta 11}$ mutant the mitochondria and the axoneme
324 detached from each other, and multiple mitochondrial derivatives (highlighted in orange and yellow)
325 attached to one axoneme (green). Mitochondria fused, enlarged (blue arrowheads) and detached (arrow)
326 from the axoneme and disintegrated axonemes with microtubule bundles and the axial membrane opening
327 is characteristic of *Grip163*$^{\Delta 11}$ mutant cyst (black arrowheads) **(g, h)**. (scale bars: A-E 2 μm, F-H 500 nm)
328

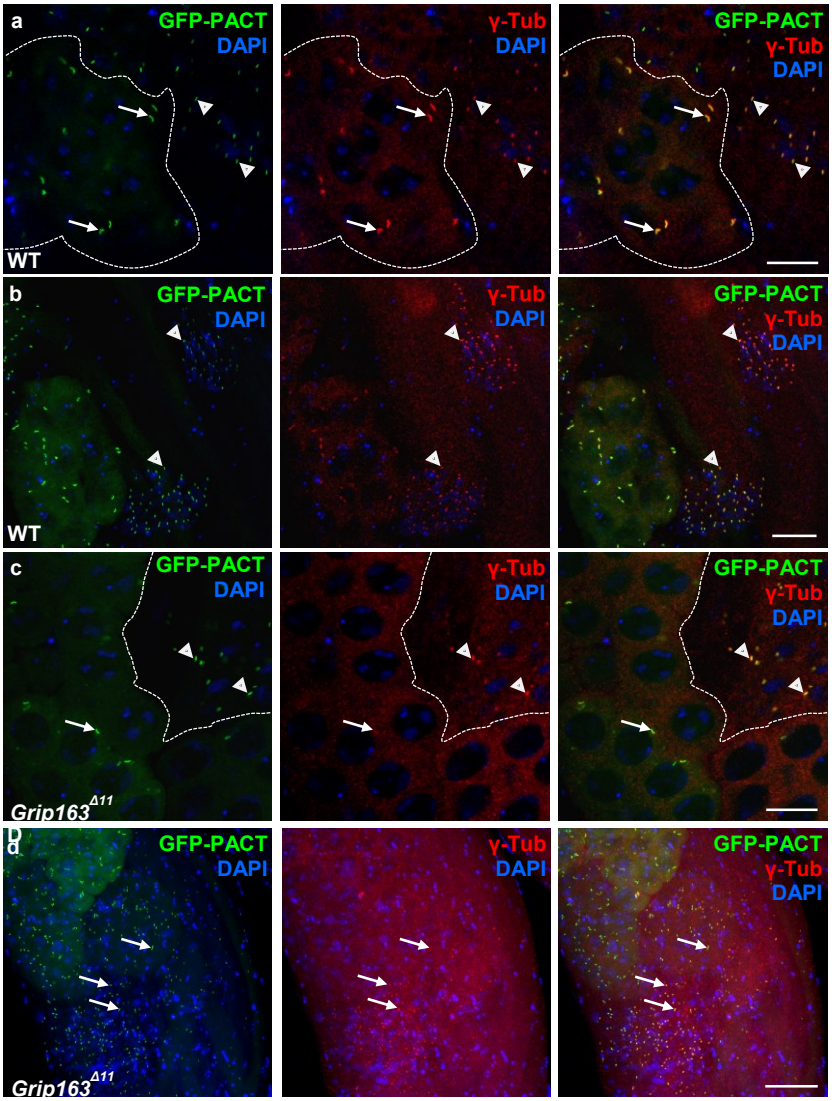

Figure 3: Mislocalization of centrosomal markers in *Grip163$^{\Delta 11}$*mutant

(a-b) GFP-PACT (green) and γ-tubulin (red) are colocalizing on the centrosome (arrows) and basal body (arrowheads) in WT spermatocytes and spermatids **(a, b)**. γ-tubulin, but not GFP-PACT centrosomal localization is affected in *Grip163$^{\Delta 11}$* mutant spermatocytes. In the round spermatids, GFP-PACT and γ-tubulin are colocalised **(c)**, but the post-meiotic elongating cysts are disorganized with scattered basal bodies. **(d)**. (scale bars: 20 µm)

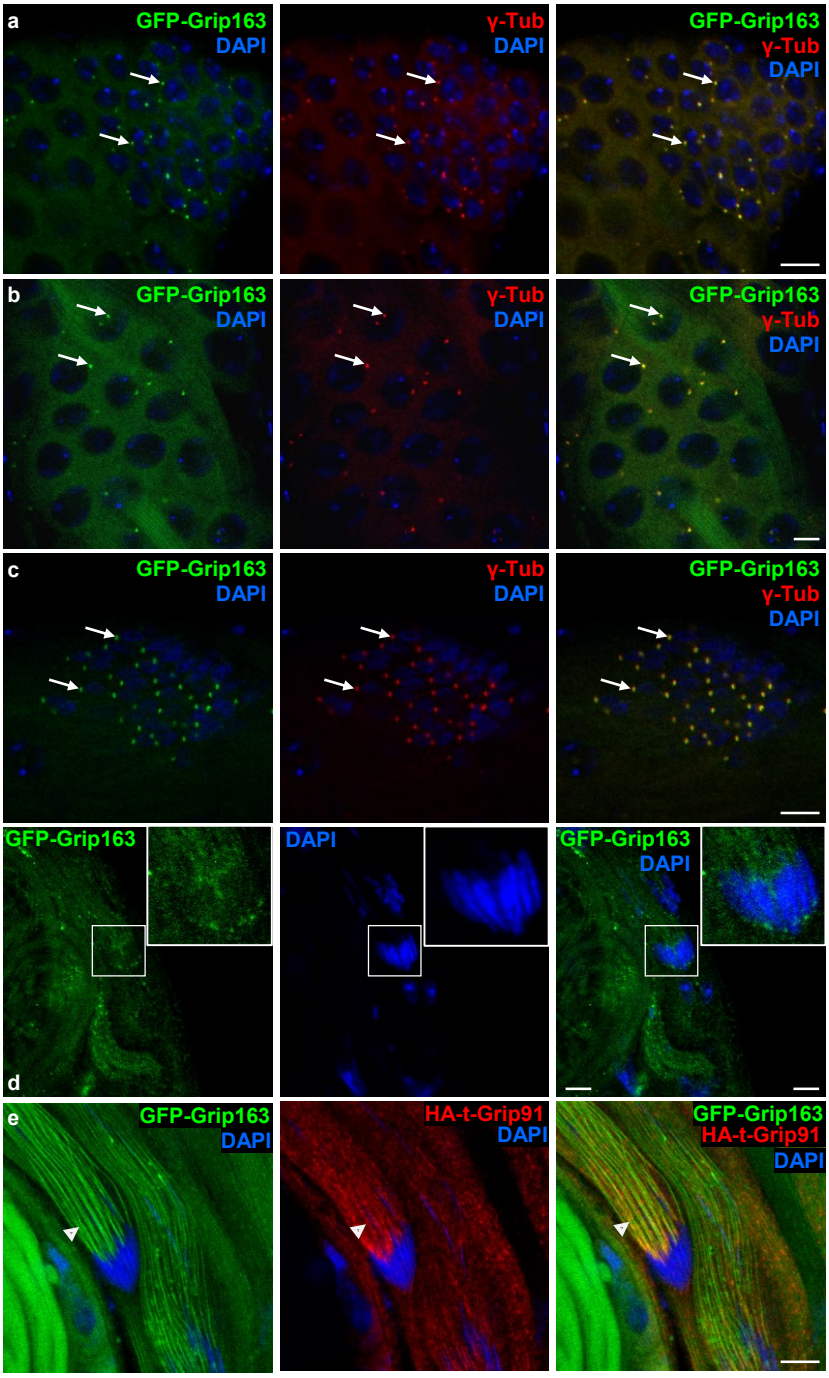

Figure 4: Localization of GFP-Grip163 during spermatogenesis.
(a-c) The endogenously tagged GFP-Grip163 colocalizes with γ-tubulin at the centrosome and the basal body throughout spermatogenesis (arrows). **(d, e)** GFP-Grip163 localizes additionally to the apical tip of the elongating nuclei **(d, inset)**, near the elongating mitochondria (arrowheads) **(e)** with overlapping localization with the t-γ-TuRC represented by HA-t-Grip91 **(e)**. (scale bars: 10 µm)

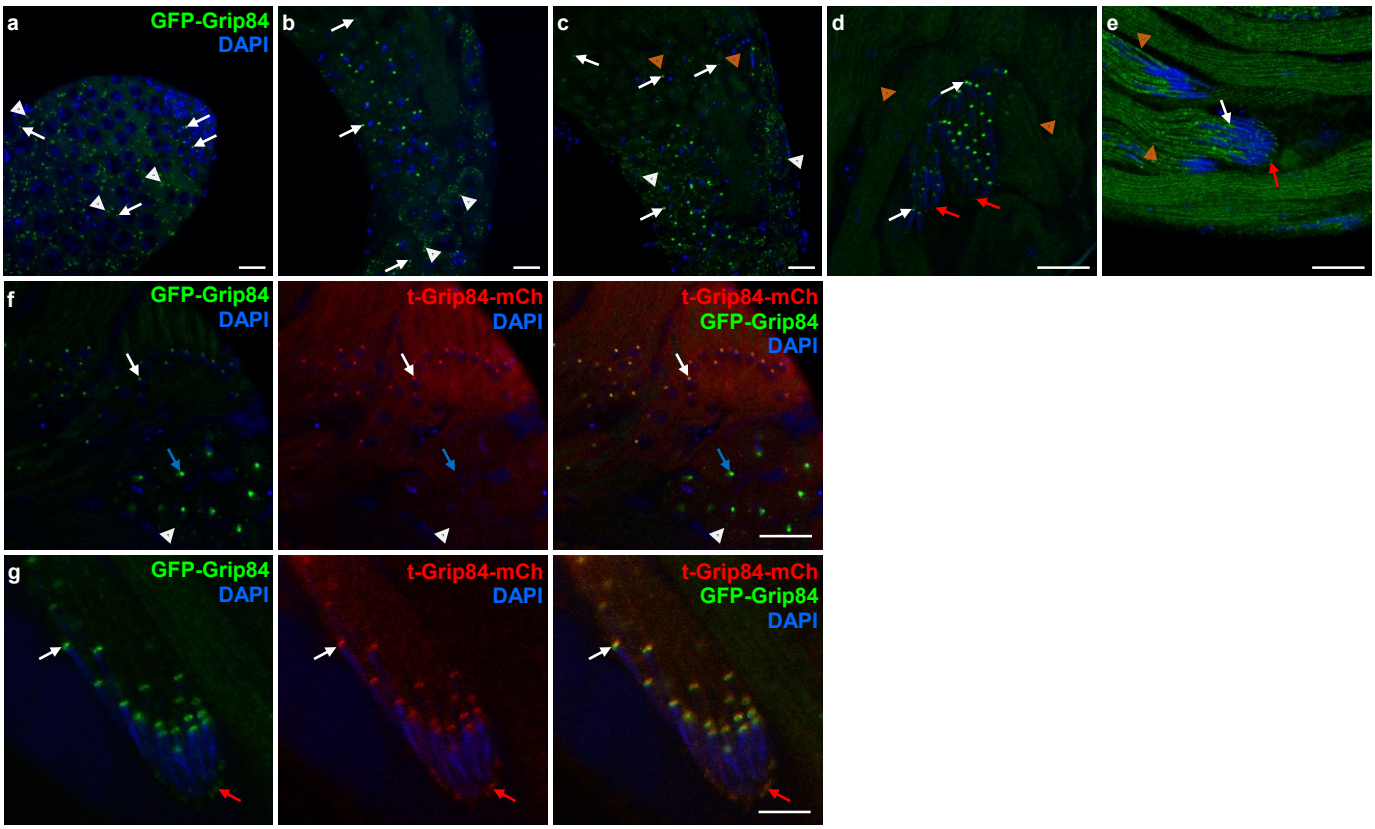

Figure 5: Localization of GFP-Grip84 during spermatogenesis.
(A-E) In vivo tagged GFP-Grip84 localizes both to the centrosome (**A**) and the basal body (**B**, **C**) (white arrows) and in the post-meiotic elongating cyst GFP-Grip84 localizes also to the apical tip of the elongating nuclei (**D**) (red arrows). Additionally, it is localized surrounding the elongating mitochondria (**C**, **D**) (orange arrowheads). Golgi-like localization of GFP-Grip84 was observed in spermatocytes (**C**) (white arrowheads). **(F, G)** GFP-Grip84 localizes to the centrosome before meiosis (blue arrows) and shows overlapping localization with t-Grip84-mCh at the basal body (white arrows) and the apical tip of the elongating nuclei (red arrows) in the post-meiotic spermatids (Scale bars: 20 µm).

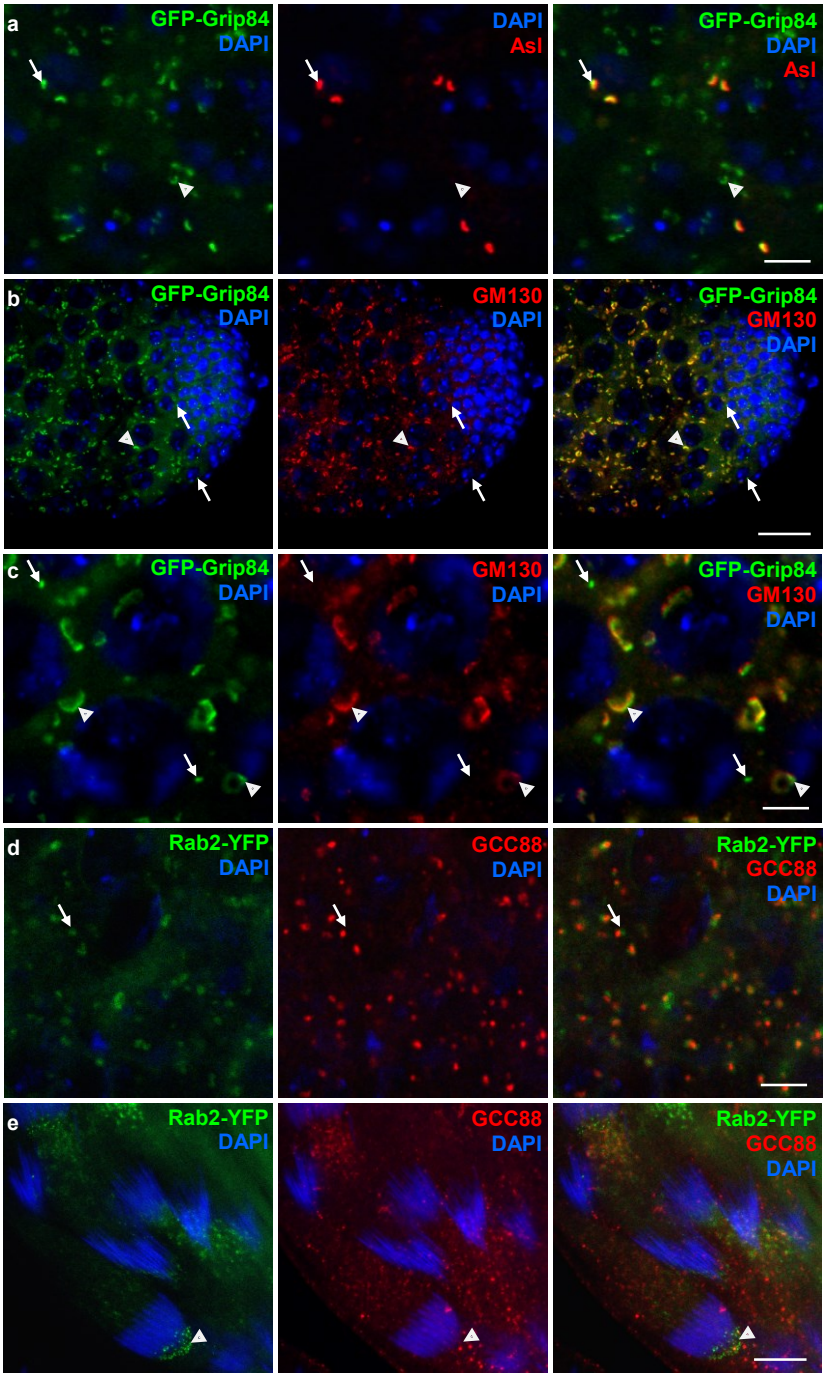

Figure 6: γ-TuSC protein GFP-Grip84 is localizing to the Golgi in spermatocytes

(A) GFP-Grip84 colocalizes with centrosomal protein Asl (anti-Asl, white arrow) and also to the Golgi apparatus (white arrowhead). **(B, C)** GFP-Grip84 colocalizes with antibody-stained *cis*-Golgi marker GM130 in the spermatocytes (arrowheads). **(D, E)** Rab2-YFP localizes to the Golgi (arrow) in spermatocytes visualised by the *trans*-Golgi marker GCC88 and also to the apical end of the elongating nuclei (arrowhead). (Scale bars: A, C, D 10 µm, B, E20 µm).

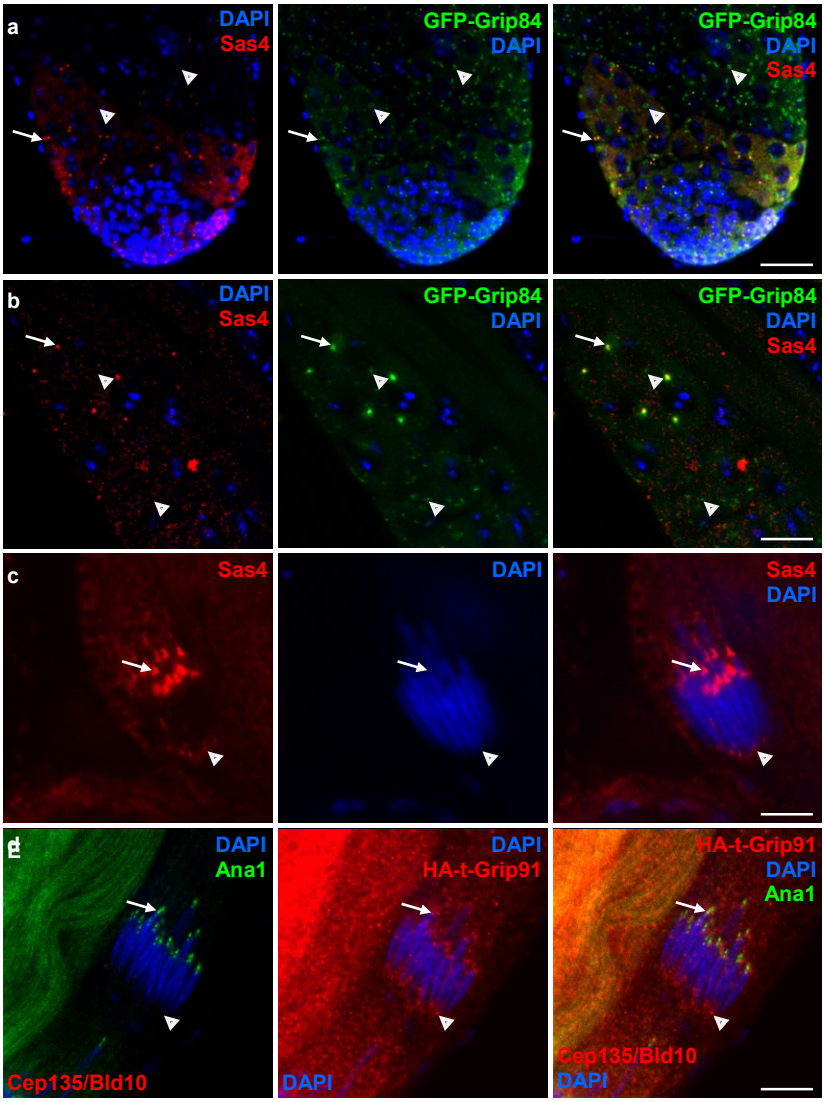

Figure 7: Sas4 is a component of the ncMTOC at the apical tip of the elongating nuclei
(A, B) Antibody-stained Sas4 (red) colocalizes with the endogenous tag GFP-Grip84 at the centrosome (arrows) but not on the Golgi (arrowheads) in the spermatocytes. **(C)** Sas4 (red) is localizing to the basal body of the elongating spermatids (arrows) and additionally to the apical tip of the nuclei (arrowheads). **(D)** Antibody-stained Ana1 localizes only to the basal body (arrows) of the elongating spermatids, while the t-γ-TuRC component HA-t-Grip91 localizes to the basal body(arrow) and the apical tip (arrowheads) of the elongating spermatids. (Scale bars: 20 µm).

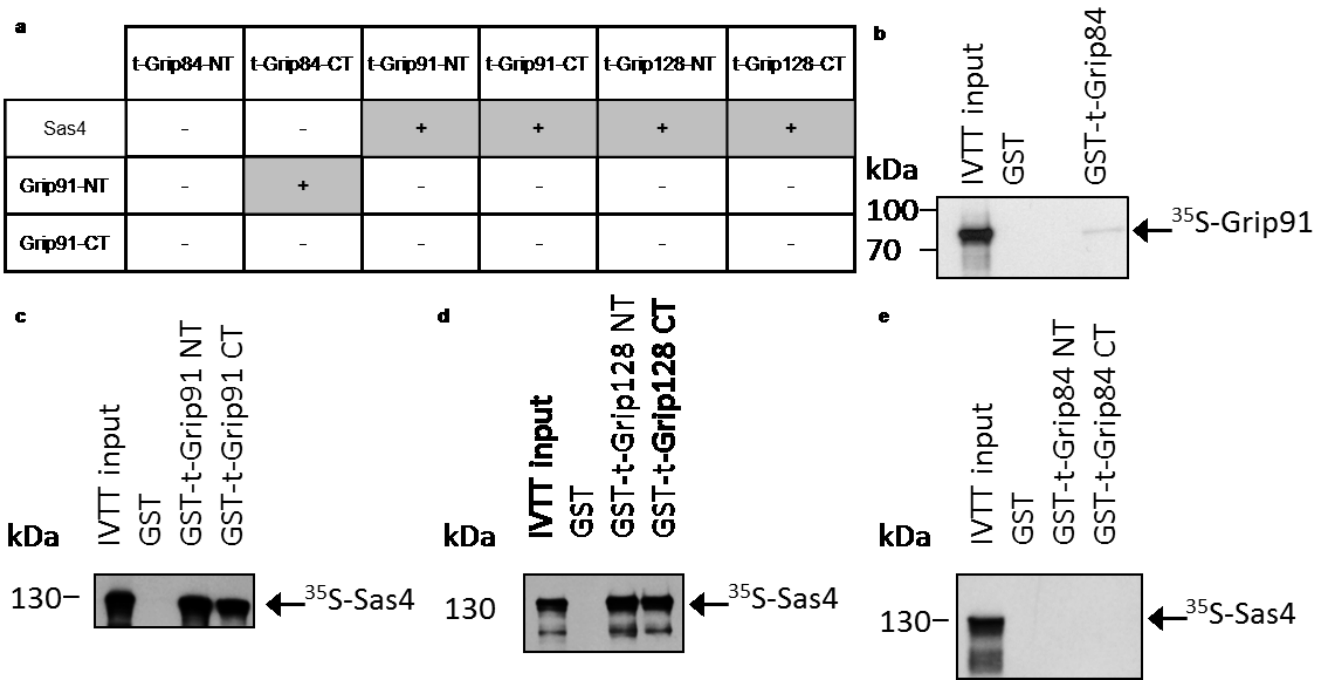

Figure 8: Interactions of t-γ-TuRC proteins with Sas4 and the canonical Grip91.
(A) Summary of Y2H analysis of the N- or C-terminal parts of t-γ-TuRC proteins (as indicated in the table) with Sas4, and the N- or C-terminal parts of Grip91, respectively. **(B-E)** Autoradiographic images showing the presence or absence of interaction between purified and immobilised GST-t-TuRC protein fragments and ^{35}S-labelled Sas4 or Grip91, synthesized by *in vitro* transcription-translation (IVTT) reaction.

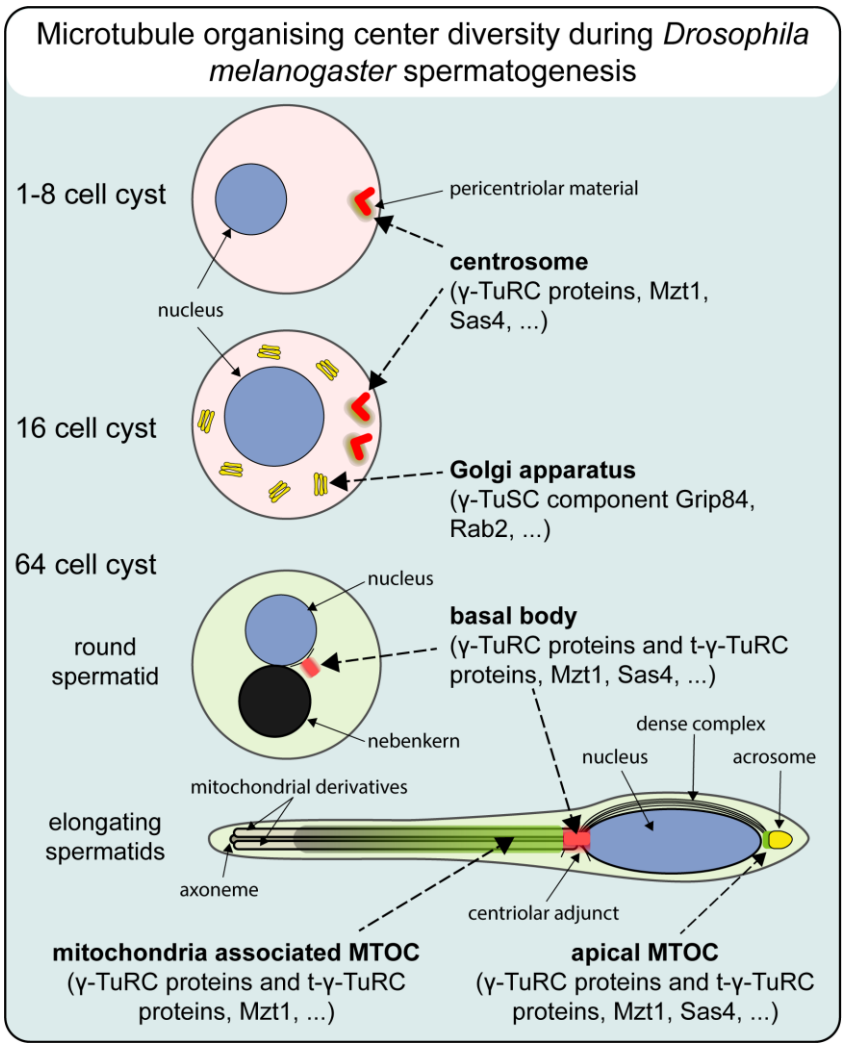

Figure 9: Summary of localization of γ-TuRC/t-γ-TuRC protein containing MTOCs during different stages of spermatogenesis.

392 **Materials and Methods**

393 **Fly stocks, mutants, and fertility test**

394 Flies were maintained on cornmeal agar medium at 25˚C in standard laboratory conditions. Fly stocks
395 used in this study were obtained from Bloomington Drosophila Stock Center, except stated otherwise.
396 w^{1118} used as wild-type control (3605, BDSC), *P{DJ-GFP.S}AS1/CyO*. The β2-tubulin-GFP line was
397 provided by David M. Glover. GFP-PACT line was obtained from Jordan Raff's and [26]. HA-t-Grip91 and
398 t-Grip84-mCh were described before (Alzyoud et al., 2021).

399 To establish the mutant allele $Grip163^{\Delta 11}$ the pCFD5-Grip163-gRNA line was crossed with vas-Cas9
400 source line to generate deletion in *Grip163*. The deletions were identified by *Grip163* specific PCR and
401 further confirmed by direct sequencing. $Grip163^{\Delta 11}$ line was established and used for further analysis.

402 To establish the genomic tagged lines of *Grip84* and *Grip163* pCFD5-Grip84-gRNA and pCFD5-
403 Grip163-gRNA lines were crossed with the vas-Cas9 source lines , w[1118]; PBac{y[+mDint2]
404 GFP[E.3xP3]=vas-Cas9}VK00027 (BL51324), y[1] M{RFP[3xP3.PB] GFP[E.3xP3]=vas-Cas9}ZH-2A
405 w[1118]/FM7c (BL51323) respectively, progeny of this cross were injected with the homology arm
406 carrying pJET1.2 plasmid (Thermo Fisher Scientific). Transgenic candidates were identified by gene
407 specific PCR and confirmed by sequencing of the insertion sites. For fertility tests, individual males were
408 crossed with three w^{1118} virgin females. After 3 days the parents were removed and 14 days after crossing,
409 the hatched progeny was counted in every tube. Experiments were repeated 4 times with > 10 males per
410 condition.

411 **DNA constructs**

412 To make the genomic GFP-Grip84, and GFP-Grip163 line, annealed oligos of the sgRNAs
413 (ATCCTTGAGCGGCTACCGCT), (GTGCTTCTCCGGTCCAGGCT) for Grip84 and Grip163
414 respectively were cloned into pCFD5 vector (Addgene, 112645) at Bbs1 restriction site using HiFi DNA
415 Assembly Master Mix (E2621S, NEB) [46]. To establish the homology arms 1534bp upstream, 1529bp
416 downstream, 1515bp upstream and 1738bp downstream of the intended GFP insertion site for Grip84 and
417 Grip163 respectively in addition to GFP were amplified using High fidelity DNA polymerase. The
418 purified PCR products were cloned into pJET1.2 plasmid (Thermo Fisher Scientific) using HiFi DNA
419 Assembly Master Mix (E2621S, NEB) [46]. GFP sequence was introduced 187bp upstream for Grip84, and
420 229bp upstream of the Grip163 sgRNA. Stable transgenic lines were established as described in Port et
421 al. [47]; [48].

422 For Y2H analysis t-Grip84 (1-399 aa N-term, 400-728 aa C-term), t-Grip128 (1-550 aa N-term, 551-975
423 aa C-term), full-length were cloned into pGAD424. full-lengths of Sas4, and t-Grip91s (1-966 aa N-term,
424 967-1932 aa C-term) were cloned into pGBT9, using HiFi DNA Assembly Master Mix (E2621S, NEB).
425 To generate GST-tagged bait proteins for the *in vitro* pull-down assay, full-length Grip84, N- and C-
426 terminal parts of t-Grip84, t-Grip91 and t-Grip128 were inserted into the pDEST15 (11802014, Thermo
427 Fisher Scientific) vector by Gateway cloning (11791-020, Thermo Fisher Scientific). Sas4 and Grip91
428 cDNAs were obtained from the *Drosophila* Gold collection (DGRC) and inserted into the pDEST17
429 plasmid (11803012, Thermo Fisher Scientific) by Gateway cloning. Oligonucleotide primers used in
430 cloning are listed in **(S. Table 1)**.

431 **Staining and microscopy**

432 Preparation and staining of tests with formaldehyde or methanol:acetone fixation were performed as
433 described by White-Cooper *et. al* [49]. Briefly, testes were dissected and fixed in 4% formaldehyde for 25
434 minutes or semi-squashed using a coverslip on poly-L-lysine coated slides, then frozen with liquid
435 nitrogen and fixed for 5 minutes in ice-cold methanol followed by 5 minutes in acetone. After fixation
436 samples were blocked and antibodies were added, the antibodies used in the study are listed in **(S.Table**
437 **2)**. Stained samples were mounted in SlowFade Gold antifade reagent (S36967, Life Technologies).
438 Images were taken using Olympus BX51 fluorescent microscope or Olympus Fluoview Fv10i confocal
439 microscope.

440 Testes for transmission electron microscopy were dissected and fixed overnight at 4°C in 2%
441 paraformaldehyde and 2% glutaraldehyde. After rinsing in phosphate-buffered saline (PBS), the testes
442 were further fixed for 1 h in 2% OsO_4, followed by dehydration in increasing ethanol concentrations and
443 rinsing in uranyl acetate and acetone. The samples were embedded in Embed812 (Electron Microscopy
444 Sciences, Hatfield, PA, USA) then ultrathin (70 nm) sections were cut on an Ultracut S ultra-microtome
445 (Leica, Wetzlar, Germany), which were mounted on copper grids. The grids were counterstained with
446 uranyl acetate (Merck, Germany) and lead citrate (Merck, Germany) and were examined and
447 photographed with a JEOL JEM 1400 transmission electron microscope (JEOL, Tokyo, Japan). The
448 images were processed with the TEM Center software (JEOL, Tokyo, Japan).

449

450 **Yeast two-hybrid assay**

451 Y2H assays were carried out using the Matchmaker two-hybrid system (K1605, Clontech). One of the
452 baits pGBT9: N- and C- terminal parts of t-Grip91 and full-length γ-Tub23C was cotransformed with one

453 of the preys pGAD424: N- and C- terminal parts of t-Grip84, t-Grip91, t-Grip128, full-length Mzt1 and
454 γ-Tub23C into PJ69 yeast cells [50]. Individual colonies were streaked out on yeast synthetic double drop-
455 out plates that lacked tryptophan and leucine (Y0750, Merck), after growing, they were inoculated on
456 quadruple dropout plates lacking (tryptophan, leucine, histidine, and adenine (Y2021, Merck) contains
457 10mM 3-amino-1, 2, 4-aminotrizole (3-AT) (A8056, Sigma).

458 **Recombinant protein production**

459 Recombinant GST-tagged bait proteins were expressed, purified and immobilized onto glutathione
460 sepharose beads as described previously [51].

461 **Coupled *in vitro* transcription-translation (IVTT) reaction and *in vitro* binding assay**

462 ^{35}S-methionine-labelled prey proteins (Grip91, Sas4) were produced *in vitro* using the TnT T7 Quick
463 Coupled IVTT kit (L1170, Promega). The detailed protocol of the GST-IVTT binding assay is described
464 previously [52].

465 **Quantification and statistical analysis**

466 Data analysis and graph production was done using Origin 9.0 (OriginLab Corporation, Northampton,
467 MA, USA). One-way ANOVA followed by Tukey's HSD test was used to comparisons between WT and
468 mutants.

469

470 **Acknowledgements**

471 We are grateful to the members of RS group. We are indebted to David M. Glover, Helen White-Cooper,
472 Sean Munro and Jordan Raff for fly stocks and reagents; for the Drosophila Genomics Resource Center
473 (supported by NIH grant 2P40OD010949) for cDNA clones and to Ferenc Jankovics for critical reading
474 of the manuscript.

475

476 **Funding**

477 This work was supported by Hungarian Science Foundation (K132155) to RS and by the Hungarian
478 Academy of Sciences (Lendület Program Grant (LP2017-7/2017)) to ZL.

479

480 References

481

482 1. Muroyama, A., Seldin, L. & Lechler, T. Divergent regulation of functionally distinct γ-tubulin
483 complexes during differentiation. *J. Cell Biol.* **213**, 679–692 (2016).
484 2. Muroyama, A. & Lechler, T. Microtubule organization, dynamics and functions in
485 differentiated cells. *Dev. Camb. Engl.* **144**, 3012–3021 (2017).
486 3. Tillery, M., Blake-Hedges, C., Zheng, Y., Buchwalter, R. & Megraw, T. Centrosomal and
487 Non-Centrosomal Microtubule-Organizing Centers (MTOCs) in Drosophila melanogaster.
488 *Cells* **7**, 121 (2018).
489 4. Desai, A. & Mitchison, T. J. Microtubule polymerization dynamics. *Annu. Rev. Cell Dev.*
490 *Biol.* **13**, 83–117 (1997).
491 5. Moritz, M., Braunfeld, M. B., Guénebaut, V., Heuser, J. & Agard, D. A. Structure of the γ-
492 tubulin ring complex: A template for microtubule nucleation. *Nat. Cell Biol.* **2**, 365–370
493 (2000).
494 6. Zheng, Y., Wong, M. L., Alberts, B. & Mitchison, T. Nucleation of microtubule assembly by
495 a gamma-tubulin-containing ring complex. *Nature* **378**, 578–583 (1995).
496 7. Fry, A. M., Sampson, J., Shak, C. & Shackleton, S. Recent advances in pericentriolar
497 material organization: ordered layers and scaffolding gels. *F1000Research* **6**, 1622 (2017).
498 8. Kollman, J. M., Merdes, A., Mourey, L. & Agard, D. A. Microtubule nucleation by γ-tubulin
499 complexes. *Nat. Rev. Mol. Cell Biol.* **12**, 709–721 (2011).
500 9. Oegema, K. *et al.* Characterization of Two Related Drosophila γ-tubulin Complexes that
501 Differ in Their Ability to Nucleate Microtubules. *J. Cell Biol.* **144**, 721–733 (1999).
502 10. Gunawardane, R. N. *et al.* Characterization and reconstitution of Drosophila gamma-tubulin
503 ring complex subunits. *J. Cell Biol.* **151**, 1513–1524 (2000).
504 11. Vérollet, C. *et al.* Drosophila melanogaster gamma-TuRC is dispensable for targeting
505 gamma-tubulin to the centrosome and microtubule nucleation. *J. Cell Biol.* **172**, 517–528
506 (2006).
507 12. Tokuyasu, K. T. Dynamics of spermiogenesis in Drosophila melanogaster. VI. Significance
508 of ‘onion’ nebenkern formation. *J. Ultrastruct. Res.* **53**, 93–112 (1975).
509 13. Avasthi, P. & Marshall, W. F. Stages of ciliogenesis and regulation of ciliary length. *Differ.*
510 *Res. Biol. Divers.* **83**, S30-42 (2012).
511 14. Laurinyecz, B. *et al.* Sperm-Leucylaminopeptidases are required for male fertility as
512 structural components of mitochondrial paracrystalline material in Drosophila melanogaster
513 sperm. *PLoS Genet.* **15**, 1–24 (2019).
514 15. Alzyoud, E., Vedelek, V., Réthi-Nagy, Z., Lipinszki, Z. & Sinka, R. Microtubule Organizing
515 Centers Contain Testis-Specific γ-TuRC Proteins in Spermatids of Drosophila. *Front. Cell*
516 *Dev. Biol.* **9**, 727264 (2021).
517 16. Chen, J. V., Buchwalter, R. A., Kao, L.-R. & Megraw, T. L. A Splice Variant of Centrosomin
518 Converts Mitochondria to Microtubule-Organizing Centers. *Curr. Biol. CB* **27**, 1928-1940.e6
519 (2017).
520 17. Tovey, C. A. *et al.* γ-TuRC Heterogeneity Revealed by Analysis of Mozart1. *Curr. Biol. CB*
521 **28**, 2314-2323.e6 (2018).
522 18. Vedelek, V. *et al.* Analysis of Drosophila melanogaster testis transcriptome 06 Biological
523 Sciences 0604 Genetics. *BMC Genomics* **19**, 1–19 (2018).

524 19. Wasbrough, E. R. *et al.* The Drosophila melanogaster sperm proteome-II (DmSP-II). *J.*
525 *Proteomics* **73**, 2171–2185 (2010).
526 20. Barbosa, V., Yamamoto, R. R., Henderson, D. S. & Glover, D. M. Mutation of a Drosophila
527 gamma tubulin ring complex subunit encoded by discs degenerate-4 differentially disrupts
528 centrosomal protein localization. *Genes Dev.* **14**, 3126–3139 (2000).
529 21. Colombié, N. *et al.* The Drosophila gamma-tubulin small complex subunit Dgrip84 is
530 required for structural and functional integrity of the spindle apparatus. *Mol. Biol. Cell* **17**,
531 272–282 (2006).
532 22. Vogt, N., Koch, I., Schwarz, H., Schnorrer, F. & Nüsslein-Volhard, C. The gammaTuRC
533 components Grip75 and Grip128 have an essential microtubule-anchoring function in the
534 Drosophila germline. *Dev. Camb. Engl.* **133**, 3963–3972 (2006).
535 23. Bre, M. H. *et al.* Axonemal tubulin polyglycylation probed with two monoclonal antibodies:
536 widespread evolutionary distribution, appearance during spermatozoan maturation and
537 possible function in motility. *J. Cell Sci.* **109**, 727–738 (1996).
538 24. Bärenz, F., Mayilo, D. & Gruss, O. J. Centriolar satellites: Busy orbits around the
539 centrosome. *Eur. J. Cell Biol.* **90**, 983–989 (2011).
540 25. Gupta, H. *et al.* SAS-6 Association with γ-Tubulin Ring Complex Is Required for Centriole
541 Duplication in Human Cells. *Curr. Biol.* **30**, 2395-2403.e4 (2020).
542 26. Martinez-Campos, M., Basto, R., Baker, J., Kernan, M. & Raff, J. W. The Drosophila
543 pericentrin-like protein is essential for cilia/flagella function, but appears to be dispensable
544 for mitosis. *J. Cell Biol.* **165**, 673–683 (2004).
545 27. Bourbon, H.-M. *et al.* A P-insertion screen identifying novel X-linked essential genes in
546 Drosophila. *Mech. Dev.* **110**, 71–83 (2002).
547 28. Dzhindzhev, N. S. *et al.* Asterless is a scaffold for the onset of centriole assembly. *Nature*
548 **467**, 714–718 (2010).
549 29. Allan, V. J., Thompson, H. M. & McNiven, M. A. Motoring around the Golgi. *Nat. Cell Biol.*
550 **4**, E236–E242 (2002).
551 30. Kondylis, V. & Rabouille, C. The Golgi apparatus: Lessons from Drosophila. *FEBS Lett.*
552 **583**, 3827–3838 (2009).
553 31. Gillingham, A. K., Sinka, R., Torres, I. L., Lilley, K. S. & Munro, S. Toward a
554 Comprehensive Map of the Effectors of Rab GTPases. *Dev. Cell* **31**, (2014).
555 32. Morohoshi, A. *et al.* FAM71F1 binds to RAB2A and RAB2B and is essential for acrosome
556 formation and male fertility in mice. *Development* **148**, dev199644 (2021).
557 33. Riparbelli, M. G., Persico, V. & Callaini, G. The Microtubule Cytoskeleton during the Early
558 Drosophila Spermiogenesis. *Cells* **9**, 2684 (2020).
559 34. Fu, J. *et al.* Conserved molecular interactions in centriole-to-centrosome conversion. *Nat.*
560 *Cell Biol.* **18**, 87–99 (2016).
561 35. Gopalakrishnan, J. *et al.* Tubulin nucleotide status controls Sas-4-dependent pericentriolar
562 material recruitment. *Nat. Cell Biol.* **14**, 865–873 (2012).
563 36. Galletta, B. J. *et al.* A centrosome interactome provides insight into organelle assembly and
564 reveals a non-duplication role for Plk4. *Nat. Commun.* **7**, 12476 (2016).
565 37. Gopalakrishnan, J. *et al.* Sas-4 provides a scaffold for cytoplasmic complexes and tethers
566 them in a centrosome. *Nat. Commun.* **2**, 359 (2011).
567 38. Guruharsha, K. G. *et al.* A Protein Complex Network of Drosophila melanogaster. *Cell* **147**,
568 690–703 (2011).

39. Dzhindzhev, N. S. *et al.* Plk4 phosphorylates Ana2 to trigger Sas6 recruitment and procentriole formation. *Curr. Biol. CB* **24**, 2526–2532 (2014).
40. Efimov, A. *et al.* Asymmetric CLASP-dependent nucleation of non-centrosomal microtubules at the trans-Golgi network. *Dev. Cell* **12**, 917–930 (2007).
41. Becker, R. *et al.* Myogenin controls via AKAP6 non-centrosomal microtubule-organizing center formation at the nuclear envelope. *eLife* **10**, e65672 (2021).
42. Brodu, V., Baffet, A. D., Le Droguen, P.-M., Casanova, J. & Guichet, A. A developmentally regulated two-step process generates a noncentrosomal microtubule network in Drosophila tracheal cells. *Dev. Cell* **18**, 790–801 (2010).
43. Mukherjee, A., Brooks, P. S., Bernard, F., Guichet, A. & Conduit, P. T. Microtubules originate asymmetrically at the somatic golgi and are guided via Kinesin2 to maintain polarity within neurons. *eLife* **9**, e58943 (2020).
44. Lund, V. K., Madsen, K. L. & Kjaerulff, O. Drosophila Rab2 controls endosome-lysosome fusion and LAMP delivery to late endosomes. *Autophagy* **14**, 1520–1542 (2018).
45. Fári, K., Takács, S., Ungár, D. & Sinka, R. The role of acroblast formation during *Drosophila* spermatogenesis. *Biol. Open* **5**, 1102–1110 (2016).
46. Gibson, D. G. *et al.* Enzymatic assembly of DNA molecules up to several hundred kilobases. *Nat. Methods* **6**, 343–345 (2009).
47. Port, F. & Bullock, S. L. Creating Heritable Mutations in Drosophila with CRISPR-Cas9. in *Methods in Molecular Biology* vol. 1478 145–160 (2016).
48. Port, F., Chen, H. M., Lee, T. & Bullock, S. L. Optimized CRISPR/Cas tools for efficient germline and somatic genome engineering in Drosophila. *Proc. Natl. Acad. Sci. U. S. A.* **111**, (2014).
49. White-cooper, H. Analysis of Meiosis and Morphogenesis. *Drosoph. Cytogenet. Protoc.* **247**, 468 (2004).
50. James, P., Halladay, J. & Craig, E. A. Genomic Libraries and a Host Strain Designed for Highly Efficient Two-Hybrid Selection in Yeast. *Genetics* **144**, 1425–1436 (1996).
51. Karman, Z. *et al.* Novel perspectives of target-binding by the evolutionarily conserved PP4 phosphatase. *Open Biol.* **10**, 200343 (2020).
52. Réthi-Nagy, Z., Ábrahám, E. & Lipinszki, Z. GST-IVTT pull-down: a fast and versatile in vitro method for validating and mapping protein-protein interactions. *FEBS Open Bio* **12**, 1988–1995 (2022).
53. Sinka, R., Gillingham, A. K., Kondylis, V. & Munro, S. Golgi coiled-coil proteins contain multiple binding sites for Rab family G proteins. *J. Cell Biol.* **183**, 607–15 (2008).

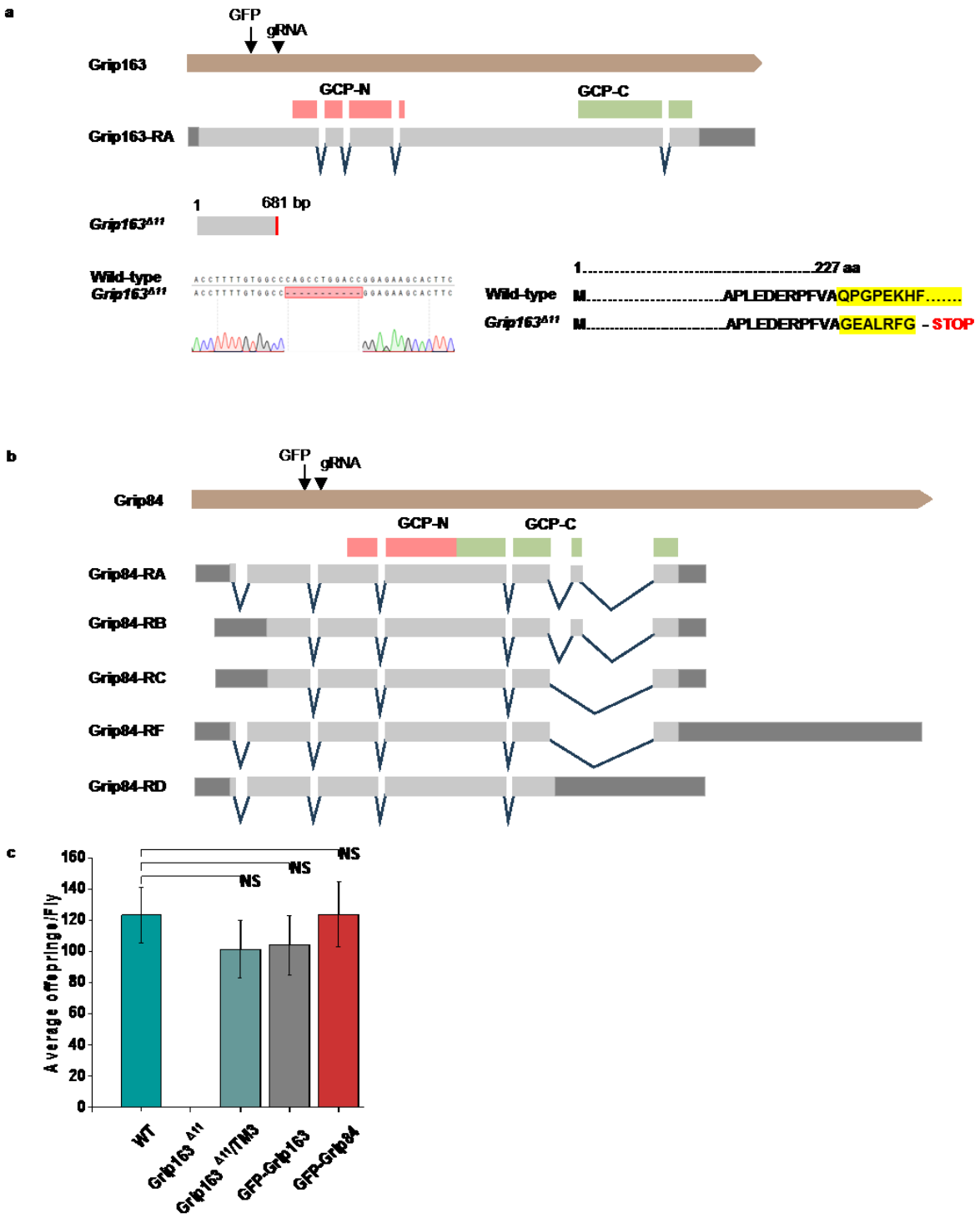

Supplementary Figure 1: Structural arrangement of *Grip163* and *Grip84* genes and transcripts. **(A)** Gene structure, transcript composition and protein domains (GCP-N, GCP-C) of Grip163. gRNA position (11,997,349..11,997,371 [+]) and the position of the *in vivo* inserted GFP tag (11,997,601 [-]) is labelled. *Grip163*$^{\Delta 11}$ mutant has an 11bp deletion (11,997,369..11,997,359). The DNA and the protein sequences surrounding the deletion are shown. **(B)** Gene structure of Grip84 with the sites of gRNA (19,564,635..19,564,657 [-]) and the GFP tag (19,564,845 [-]). The inserted GFP tag labels all five Grip84

612 isoforms **(C)** Graph represents the fertility test of WT (n=14), *Grip163*$^{\Delta 11}$ (n=6), *Grip163*$^{\Delta 11}$*/Cyo* (n= 12),
613 GFP-Grip84 (n=12) and GFP-Grip163 (n=15) males. Statistical significance was tested by one-way
614 ANOVA.

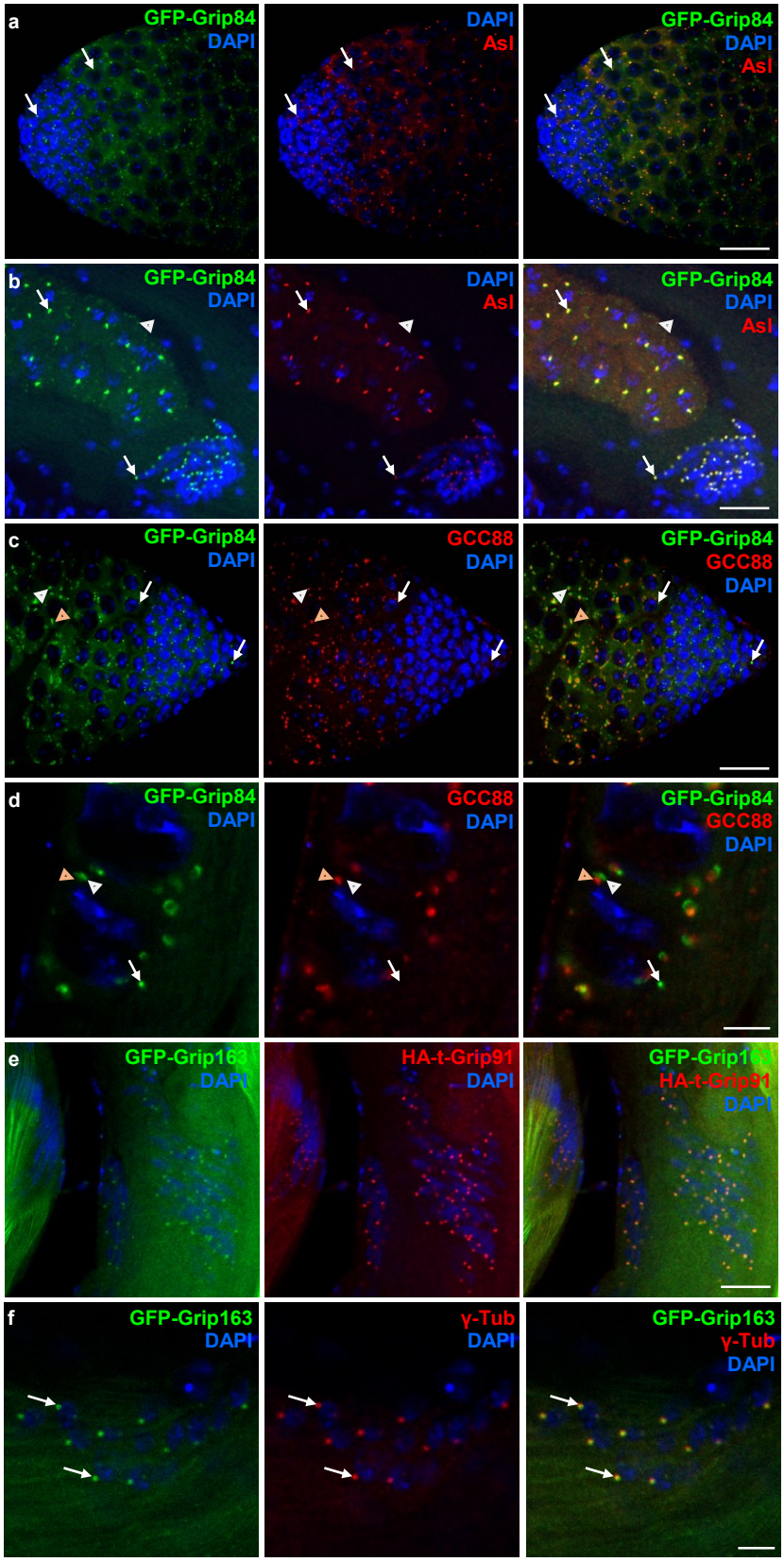

615

616 **Supplementary Figure 2: Grip84 and Grip163 localization during spermatogenesis**.

(A-D) The endogenous tag GFP-Grip84 colocalizes with antibody-stained Asl (red) at the (**A**) centrosome (arrow) and the (**B**) basal body (arrow) of the spermatocytes and the spermatids, but not with the Golgi localized GFP-Grip84 (arrowhead). **(C, D)** GFP-Grip84 localizes adjacent to antibody-stained *trans*-Golgi marker GCC88 (arrowheads) and to the centrosome (arrow) in spermatocytes. **(E, F)** in vivo tagged GFP-Grip163 colocalizes with the testis-specific HA-t-Grip91 (arrow) in the post-meiotic stages. (Scale bars: 20 µm).

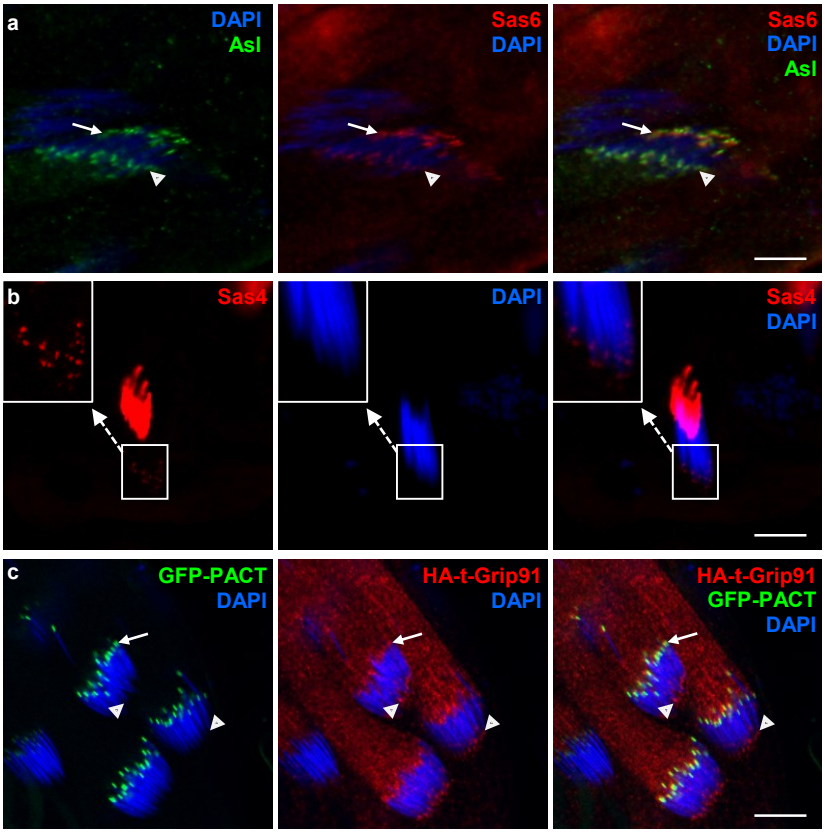

Supplementary Figure 3: Localization of centrosomal and basal body component proteins in spermatids.

(A, B) Asl, Sas6 and Sas4 localization to the basal body (arrow) and the apical tip (arrowhead) of elongating spermatids are visualised by immunostaining using gene-specific antibodies. **(C)** GFP-PACT localizes to the basal body (arrows) of the elongating spermatids, while the HA-t-Grip91 localizes to the basal body (arrow) and the apical tip (arrowheads) of the elongating spermatids. (Scale bars: 20 µm)

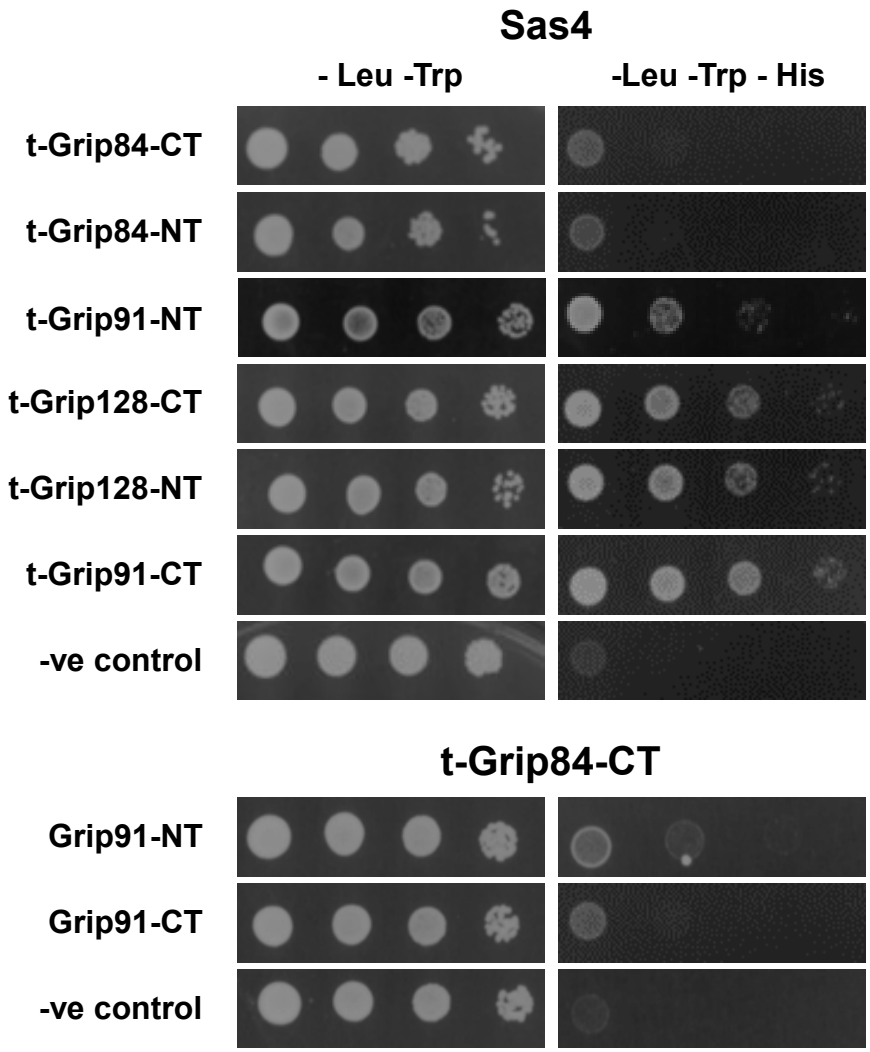

Supplementary Figure 4: Interactions tested by Yeast Two-Hybrid assay
Mated yeast was plated as 10-fold serial dilutions (left to right) on -Leu, -Trp medium that is selective for the bait and prey plasmids and -Leu, -Trp, -His, -Ade medium that is selective for the bait, prey, and the interaction between the tested proteins. Negative control (-control) is the empty prey with the corresponding bait vector.

638 **Supplementary Table1 List of antibodies.**

Antibody /Dye	Dilution	Source	Identifier	Fixation method
Anti-HA (rat)	1:100	Sigma-Aldrich/Roche	Cat# 11867423001	Formaldehyde
Anti-Sas4 (rat)	1:500	[34]		Methanol-acetone
Anti-Sas6 (rat)	1:500	[39]		Methanol-acetone
GM130 (rabbit)	1:500	Abcam	ab30637	Formaldehyde
GCC88 (G. pig)	1:100	[53]		Formaldehyde
Anti-GFP (rabbit)	1:500	Thermo Fisher Scientific	Cat#A-11122	Methanol-acetone
anti-pan polyglycylated Tubulin Axo49 (mouse)	1:5000	Sigma-Aldrich/Merck	Cat# MABS276	Formaldehyde
anti-γ-Tubulin (mouse)	1:5000	Sigma-Aldrich/Merck	Cat# T6557	Formaldehyde
anti-Ana1 (rabbit)	1:5000	[34]	-	Formaldehyde
anti-Asl (rabbit)	1:1000	[28]	-	Methanol-acetone
G.pig Alexa Fluor 546 secondary	1:400	ThermoFisher	Cat# A-11074	
Mouse Alexa Fluor 488 secondary	1:400	Thermo Fisher Scientific	Cat#A-11029	
Mouse Alexa Fluor 546 secondary	1:400	Thermo Fisher Scientific	Cat#A-11030	
Mouse Alexa Fluor 633 secondary	1:400	Thermo Fisher Scientific	Cat#A-21052	
Rat Alexa Fluor 488 secondary	1:400	Thermo Fisher Scientific	Cat#A-21208	
Rat Alexa Fluor 568 secondary	1:400	Thermo Fisher Scientific	Cat#A-11081	

Rabbit Alexa Fluor 488 secondary	1:400	Thermo Fisher Scientific	Cat#A-11008	
Rabbit Alexa Fluor 546 secondary	1:400	Thermo Fisher Scientific	Cat#A-11010	
4',6-Diamidino-2-Phenylindole, Dihydrochloride (DAPI)	1 µg/ml	Thermo Fisher Scientific	Cat#D1306	

639

640 **Supplementary Table2 List and sequence of primers**

Primer Name	Primer Sequence
Grip163-gRNA-fwd	tgcagtgcttctccggtccaggct
Grip163-gRNA-rev	aaacagcctggaccggagaagcac
Grip163-1.5 kb upstream_fwd	gtgccacctgacgtctaagagatacatcccataattaccatacttacccag
Grip163-1.5 kb upstream_rev	tgctcaccatcaggggtttcagggcgcg
Grip163-GFP_fwd	gaaacccctgatggtgagcaagggcgag
Grip163-GFP_rev	gctgtagttgcttgtacagctcgtccatg
Grip163-before PAM_fwd	gctgtacaagcaactacagccatactccg
Grip163-before PAM_rev	ccaggctgtgccacaaaaggtcgttcatc
Grip163-Mutant PAM_fwd	ccttttgtggcacagcctggaccggagaag
Grip163-Mutant PAM_rev	gagttagctcactcattaggggtcaggactggacgacag
pJET1_fwd	cctaatgagtgagctaactcac
pJET1_rev	tcttagacgtcaggtggcac
Grip84-gRNA-fwd	tgcaatccttgagcggctaccgct
Grip84-gRNA-rev	aaacagcggtagccgctcaaggat
Grip84-1.5 kb upstream-fwd	ccacctgacgtctaagatgacccgctgaccatggc
Grip84-1.5 kb upstream-rev	ctcaccattacgggtgtagtgtcggattc
Grip84-GFP_fwd	cacccgtaatggtgagcaagggcgag
Grip84-GFP_rev	acaaagaccttgtacagctcgtccatg
Grip84-before PAM_fwd	gctgtacaaggtctttgtcaggcgcggc
Grip84-before PAM _rev	acagagcggtagccgctcaaggattg
Grip84-mutant PAM_fwd	cggctaccgctctgtgaccaacaaaacg
Grip84-mutant PAM_rev	ttagctcactcattagggctcgcagtgcagatcgtc
YTH Sas4_fwd	atcgccggaattcccaatgcaggaggctggcgaaag
YTH Sas4_rev	ggtcgacggatccccctaatacttggcatagtctgtgtccattatg
YTH t-Grip91-N_fw	atcgccggaattcccaatggagacgcagccatttaaaattg
YTH t-Grip91-N_rev	ggtcgacggatccccttaaactaacatagggtatcaatttcaac
YTH t-Grip91-C_fw	atcgccggaattcccaatggaaagtcttcgtgaag
YTH t-Grip91-C_rev	ggtcgacggatccccttacagtgatcttttcctttcc

YTH t-Grip84-N_fw	aaagagatcgaattcccaatgaactccgacaaatcg
YTH t-Grip84-N_rev	ggtcgacggatccccttaattgtgctcctccacc
YTH t-Grip84-C_fw	aaagagatcgaattcccaatgttgcctttacacattcg
YTH t-Grip84-C_rev	ggtcgacggatccccttaaatattggaagctatttgatcc
YTH t-Grip128-N_fw	aaagagatcgaattcccaatgcaagaggacgagag
YTH t-Grip128-N_rev	ggtcgacggatccccttatcgttcatcggtcacaatc
YTH t-Grip128-C_fw	aaagagatcgaattcccaatgacagagtacgtcttaagaaaatc
YTH t-Grip128-C_rev	ggtcgacggatccccttaaatatggccgagcaaac
GST t-Grip91-N_fw	cgacggtaccatggagacgcagccatttaaaat
GST t-Grip91-N_rev	gcggccgcttaaactaacatagggtatcaatttcaac
GST t-Grip128-N_fw	cgacggtaccatgcaagaggacgagagaca
GST t-Grip128-N_rev	gcggccgcttatcgttcatcggtcacaatc
GST t-Grip128-C_fw	cgacggtaccatgacagagtacgtcttaagaaaatc
GST t-Grip128-C_rev	gcggccgcttaaatatggccgagcaaaca
GST t-Grip84-N_fw	gaattcaaatgaactccgacaaatcggaaagtg
GST t-Grip84-N_rev	gcggccgcttaattgtgctcctccacc
GST t-Grip84-C_fw	gaattcaaatgttgcctttacacattcg
GST t-Grip84-C_rev	gcggccgcttaaatattggaagctatttgatcc

641

642